Implicit Space-Time Conservation Element and Solution Element Schemes

Sin-Chung Chang
NASA Glenn Research Center
Cleveland, Ohio 44135
e-mail: sin-chung.chang@grc.nasa.gov
Web site: http://www.grc.nasa.gov/www/microbus

Ananda Himansu
Taitech Inc. at NASA Glenn Research Center
Cleveland, Ohio 44135
e-mail: ananda.himansu@grc.nasa.gov

and

Xiao-Yen Wang
Taitech Inc. at NASA Glenn Research Center
Cleveland, Ohio 44135
e-mail: wangxy@turbot.grc.nasa.gov

Submitted for Publication in
Journal of Computational Physics

Subject classifications: 65C99, 76J99, 76L05, 76N10.

Key words: Space-Time, Flux Conservation, Conservation Element, Solution Element, Implicit, Convection, Diffusion.

Proposed running title: The Implicit CE/SE Schemes.

Proofs sent to:
Dr. S.C. Chang, MS 5-11, NASA Glenn Research Center, Cleveland, Ohio 44135.
e-mail: sin-chung.chang@grc.nasa.gov
Fax: (216) 433-5802

Abstract

Artificial numerical dissipation is an important issue in large Reynolds number computations. In such computations, the artificial dissipation inherent in traditional numerical schemes can overwhelm the physical dissipation and yield inaccurate results on meshes of practical size. In the present work, the space-time conservation element and solution element method is used to construct new and accurate implicit numerical schemes such that artificial numerical dissipation will not overwhelm physical dissipation. Specifically, these schemes have the property that numerical dissipation vanishes when the physical viscosity goes to zero. These new schemes therefore accurately model the physical dissipation even when it is extremely small. The new schemes presented are two highly accurate implicit solvers for a convection-diffusion equation. The two schemes become identical in the pure convection case, and in the pure diffusion case. The implicit schemes are applicable over the whole Reynolds number range, from purely diffusive equations to convection-dominated equations with very small viscosity. The stability and consistency of the schemes are analysed, and some numerical results are presented. *It is shown that, in the inviscid case, the new schemes become explicit and their amplification factors are identical to those of the Leapfrog scheme. On the other hand, in the pure diffusion case, their principal amplification factor becomes the amplification factor of the Crank-Nicolson scheme.*

1 Introduction

The method of space-time conservation element and solution element (the CE/SE method, for short) is a new numerical discretization method for solving conservation laws [1-14]. It aims to overcome the limitations of the established methods, and is designed to be a mathematically simple yet general, accurate and robust method for solving conservation laws. The emphasis is on the simulation of the integral forms of the laws, rather than the differential forms. This allows for better simulation of regions of rapid change, such as shocks and boundary layers, where the numerical solution is not smooth. The method has been developed on the basis of local and global flux conservation in a space-time domain, in which space and time are treated in a unified manner. Derived properties of the conservation laws, such as the characteristics and the shock-jump conditions, are not used in the construction of the method. For problems in multiple spatial dimensions, the method is genuinely multidimensional and is fully compatible with unstructured meshes [2, 4]. The CE/SE method was first published in this journal in 1995 [1]. The generalization to multiple spatial dimensions appeared in this journal in 1999 [2]. The Introduction section of [1] begins with a lengthy discussion that focuses more on physics than on numerics. From this discussion, readers can understand (i) the considerations that motivate the new method, and (ii) the key differences that separate it from the established methods.

By using a set of design principles that are extracted from the discussion mentioned above, several two-level explicit schemes were constructed in [1, 10] to solve (i) the pure convection equation

$$\partial u/\partial t + a\,\partial u/\partial x = 0 \tag{1.1}$$

and (ii) the convection-diffusion equation

$$\partial u/\partial t + a\,\partial u/\partial x - \mu\,\partial^2 u/\partial x^2 = 0 \tag{1.2}$$

where the convection velocity a, and the viscosity coefficient μ (> 0) are constants. These schemes were then extended to solve the 1-D time-dependent Euler and Navier-Stokes equations of a perfect gas [1, 10]. Moreover, the above 1-D solvers of Eq. (1.1) have been generalized to their 2-D counterparts [2, 14, 12]. Because of the inherent simplicity and generality of the current method, the above multidimensional generalization is a straightforward matter. Also, as a result of the similarity in their designs, each of the above 2-D schemes shares with its 1-D version virtually the same fundamental characteristics.

In this paper we shall describe a simple and innovative approach by which accurate implicit time-marching solvers can be constructed using the CE/SE method. A portion of this work was presented in [5], and a more general version was recorded in [6]. A striking feature of this new treatment is that the modeling of the diffusion-related terms involves interpolation between neighboring mesh points while that of the convection-related term does not. As a preliminary, first we shall discuss the pros and cons of explicit and implicit schemes.

For a two-level explicit scheme, the value of a solution at any mesh point has a finite domain of dependence at the previous time level. As an example, consider a finite-difference solver for Eq. (1.1). Let u_j^n, the mesh value of u at any mesh point (j,n) (point P in Fig. 1(a)), be determined by u_{j-1}^{n-1}, u_j^{n-1}, and u_{j+1}^{n-1}. Then the domain of dependence of u_j^n at the $(n-1)$th time level contains three mesh points. Also one can see that u_j^n is dependent only on the initial data given on the line segment AB.

For an initial-value problem, such as a time-dependent Euler problem or a problem involving Eq. (1.1), the solution at any point in space-time also has a finite domain of dependence on the initial plane. As a result, explicit schemes could be ideal solvers for such a problem if they satisfy the requirement that the physical domain of dependence be a subset of the numerical domain of dependence.

On the other hand, the solution of an initial-value/boundary-value problem at any point in space-time is dependent on the initial data and the boundary data up to the time of the point under consideration. As an example, consider a problem involving Eq. (1.2). As shown in Fig. 1(b), the solution at point P is dependent on the initial/boundary data given on EC, CD, and DF where E, P, and F are at the same time level. Let this problem be solved using the explicit scheme that was explained using Fig. 1(a). Let P also be a mesh point (j,n). Then u_j^n is dependent only on the initial/boundary data given on AC, CD and DB. *It is completely independent of those data given on AE and BF.* Contrarily, if the same problem is solved using an implicit scheme, then u_j^n is dependent on the initial/boundary data given on EC, CD, and DF. In other words, the numerical domain of dependence of the implicit scheme is consistent with the physical domain of dependence of the problem under consideration.

Two observations can be made as a result of the above discussions.

(a) Generally an explicit scheme is not an ideal solver for an initial-value/boundary-value problem. Because a time-dependent Navier-Stokes problem is such a problem, the

above argument implies that an explicit scheme cannot be used to solve a time-dependent Navier-Stokes problem except for the special circumstance in which errors caused by neglecting certain initial/boundary data (such as those given on AE and BF in Fig. 1(b)) are relatively small. The factors that help achieve the above special circumstance include: (i) a small time-step size to spatial-mesh interval ratio, (ii) a small time rate of change of boundary data, and (iii) a small contribution of the viscous terms in the Navier-Stokes equations relative to that of the inertial terms. Note that condition (iii) may be met by a high-Reynolds-number flow.

(b) Generally an implicit scheme is not an ideal solver for an initial-value problem. This is because the domain of dependence of the former is greater than that of the latter and, as a result, an implicit solution tends to be contaminated by extraneous information.

2 Preliminaries

Let Eq. (1.1) be in a dimensionless form. Let $x_1 = x$ and $x_2 = t$ be considered as the coordinates of a two-dimensional Euclidean space E_2. By using Gauss' divergence theorem in the space-time E_2, it can be shown that Eq. (1.1) is the differential form of the integral conservation law

$$\oint_{S(V)} \vec{h} \cdot d\vec{s} = 0 \tag{2.1}$$

Here (i) $S(V)$ is the boundary of an arbitrary space-time region V in E_2, (ii) $\vec{h} = (au, u)$ is a current density vector in E_2, and (iii) $d\vec{s} = d\sigma\,\vec{n}$ with $d\sigma$ and $\vec{n}$, respectively, being the area and the outward unit normal of a surface element on $S(V)$. Note that (i) $\vec{h} \cdot d\vec{s}$ is the *space-time* flux of $\vec{h}$ leaving the region V through the surface element $d\vec{s}$, and (ii) all mathematical operations can be carried out as though E_2 were an ordinary two-dimensional Euclidean space.

In the following, we shall briefly review the inviscid version of the explicit a-μ scheme [1, 10]. Let Ω_1 denote the set of mesh points (j, n) in E_2 (dots in Fig. 2) where $n = 0, \pm 1, \pm 2, \pm 3, \ldots$, and, for each n, $j = n, n \pm 2, n \pm 4, \ldots$. There is a solution element (SE) associated with each $(j, n) \in \Omega_1$. Let the solution element SE(j, n) be the *space-time* region bounded by the dashed curve depicted in Fig. 3. It includes a horizontal line segment, a vertical line segment, and their immediate neighborhood.

For any $(x, t) \in$ SE(j, n), $u(x, t)$, and $\vec{h}(x, t)$, respectively, are approximated by $u^*(x, t\,; j, n)$ and $\vec{h}^*(x, t\,; j, n)$, which we shall define shortly. Let

$$u^*(x, t\,; j, n) = u_j^n + (u_x)_j^n (x - x_j) + (u_t)_j^n (t - t^n) \tag{2.2}$$

where (i) u_j^n, $(u_x)_j^n$, and $(u_t)_j^n$ are constants in SE(j, n), and (ii) (x_j, t^n) are the coordinates of the mesh point (j, n). Note that u_j^n, $(u_x)_j^n$, and $(u_t)_j^n$ can be interpreted as the numerical analogues of the values of u, $\partial u/\partial x$, and $\partial u/\partial t$ at (x_j, t^n), respectively.

We shall require that $u = u^*(x, t\,; j, n)$ satisfy Eq. (1.1) within SE(j, n), i.e.,

$$(u_t)_j^n = -a\,(u_x)_j^n \tag{2.3}$$

Combining Eqs. (2.2) and (2.3), one has

$$u^*(x,t\,;j,n) = u_j^n + (u_x)_j^n\,[(x-x_j) - a\,(t-t^n)] \quad (x,t) \in \mathrm{SE}(j,n) \tag{2.4}$$

Because $\vec{h} = (au,\, u)$, we define

$$\vec{h}^*(x,t\,;j,n) = (au^*(x,t\,;j,n),\, u^*(x,t\,;j,n)) \tag{2.5}$$

Let E_2 be divided into nonoverlapping rectangular regions (see Fig. 2) referred to as conservation elements (CEs). As depicted in Fig. 4, the CE with its top-right (top-left) vertex being the mesh point $(j,n) \in \Omega_1$ is denoted by $\mathrm{CE}_-(j,n)$ ($\mathrm{CE}_+(j,n)$). Obviously the boundary of $\mathrm{CE}_-(j,n)$ ($\mathrm{CE}_+(j,n)$) is formed by subsets of $\mathrm{SE}(j,n)$ and $\mathrm{SE}(j-1,n-1)$ ($\mathrm{SE}(j+1,n-1)$). The current approximation of Eq. (2.1) is

$$F_\pm(j,n) \stackrel{\mathrm{def}}{=} \oint_{S(CE_\pm(j,n))} \vec{h}^* \cdot d\vec{s} = 0 \tag{2.6}$$

for all $(j,n) \in \Omega_1$. In other words, the total flux leaving the boundary of any CE is zero.

Because (i) The CEs associated with Ω_1 can fill any space-time region, and (ii) the surface integration across any interface separating two neighboring CEs is evaluated using the information from a single SE, the local conservation condition Eq. (2.6) leads to a global conservation relation, i.e., *the total flux leaving the boundary of any space-time region that is the union of any combination of CEs will also vanish.*

With the aid of Eqs. (2.4)–(2.6), it can be shown that

$$F_\pm(j,n)/\Delta x = \pm(1-\nu^2)\left[(u_x^+)_j^n + (u_x^+)_{j\pm1}^{n-1}\right] + (1 \mp \nu)\left(u_j^n - u_{j\pm1}^{n-1}\right) \tag{2.7}$$

where $\nu = a\Delta t/\Delta x$ is the Courant number, and $(u_x^+)_j^n = (\Delta x/2)(u_x)_j^n$. *Note that here Δx and Δt, respectively, represent the same mesh interval and time-step size which were denoted by $\Delta x/2$ and $\Delta t/2$ in* [1, 10]. Using Eqs. (2.6) and (2.7), u_j^n and $(u_x^+)_j^n$, which are considered as *independent* unknowns at the mesh point (j,n), can be solved for in terms of $u_{j\pm1}^{n-1}$ and $(u_x^+)_{j\pm1}^{n-1}$ if $1-\nu^2 \neq 0$. It can be shown that, for all $(j,n) \in \Omega_1$,

$$\vec{q}(j,n) = Q_+\,\vec{q}(j-1,\,n-1) + Q_-\,\vec{q}(j+1,\,n-1) \quad (1-\nu^2 \neq 0) \tag{2.8}$$

Here (i) $\vec{q}(j,n)$ is the column matrix formed by u_j^n and $(u_x^+)_j^n$, and (ii)

$$Q_\pm \stackrel{\mathrm{def}}{=} (1/2)\begin{pmatrix} 1\pm\nu & \pm(1-\nu^2) \\ \mp 1 & -1\pm\nu \end{pmatrix} \tag{2.9}$$

Eq. (2.8) defines a marching scheme. Because this scheme is the special case of the a-μ scheme when $\mu = 0$, hereafter it will be referred to as the a scheme. It is the only *two-level explicit* solver of Eq. (1.1) known to the authors to be neutrally stable, i.e., free from numerical dissipation.

In the above construction of the a scheme, we use the SEs and CEs of the mesh points marked by dots in Fig. 2. A similar construction can be performed by using the mesh points marked by triangles in Fig. 2. Let Ω_2 denote the set of mesh points (j,n) in E_2 (triangles

in Fig. 2) where $n = 0, \pm 1, \pm 2, \pm 3, \ldots$, and, for each n, $j = n \pm 1, n \pm 3, n \pm 5, \ldots$. Let the SEs and CEs of Ω_2 be defined by using Figs 3 and 4 with dots replaced by triangles. Obviously (i) the CEs of Ω_2 also fill any space-time region, and (ii) the a scheme can also be constructed using the SEs and CEs of Ω_2. This new scheme is defined by Eq. (2.8) with $(j, n) \in \Omega_2$.

Before we proceed further, some intricate points related to the above constructions will be clarified with the following remarks:

(a) SE(j, n) may intersect SE(j', n') if $(j, n) \in \Omega_1$ and $(j', n') \in \Omega_2$.

(b) Let $(j, n) \in \Omega_1$. Then (i) $(j+1, n) \in \Omega_2$, and (ii) $\mathrm{CE}_+(j, n)$ and $\mathrm{CE}_-(j+1, n)$ represent the same rectangle in E_2. However, because the function $\vec{h}^*$ used in the evaluation of $F_+(j, n)$ is tied to a pair of SEs associated with Ω_1, while that used in the evaluation of $F_-(j+1, n)$ is tied to another pair of SEs associated with Ω_2, $F_+(j, n) = 0$ and $F_-(j+1, n) = 0$ represent *two completely independent flux conservation conditions.*

To prepare for the development of the implicit solver to be described in the next section, we shall combine the above two independent schemes into a single scheme. The new scheme, referred to as the dual a scheme, is defined by Eq. (2.8) with $(j, n) \in \Omega$ where $\Omega \stackrel{\text{def}}{=} \Omega_1 \cup \Omega_2$. Obviously, a solution of the dual a scheme is formed by two decoupled solutions with each being associated with a mesh that is staggered in time. Several classical schemes also have this property. Among them are the Leapfrog, the DuFort-Frankel, and the Lax schemes [15].

3 The implicit schemes

An implicit solver for Eq. (1.2), referred to as the a-$\mu(I1)$ scheme, will be discussed first in this section. Here "I" stands for "implicit", and "1" is the identification number. This discussion will be followed by a brief discussion of another implicit scheme, termed the a-$\mu(I2)$ scheme. The implicit schemes are constructed to meet two requirements given in the following discussion:

(a) With a few exceptions, numerical dissipation generally appears in a numerical solution of a time-marching problem. In other words, the numerical solution dissipates faster than the corresponding physical solution. For a nearly inviscid problem, e.g., flow at a large Reynolds number, this could be a serious difficulty because numerical dissipation may overwhelm physical dissipation and cause a complete distortion of solutions. To avoid such a difficulty, the model solver is required to have the property that *the numerical dissipation will approach zero as the physical dissipation approaches zero.*

(b) The convection term and the diffusion term in Eq. (1.2) involve the spatial derivatives of first order and second order, respectively. Thus, in a spatial region where a solution is very smooth, the diffusion term is negligible compared with the convection term. As a result, the *effective* physical domain of dependence is more or less dictated by Eq. (1.1). To prevent excessive contamination of the solution by extraneous information, *the implicit solver will be required to become an explicit solver in the limiting case in which the diffusion term vanishes.*

Because of the requirements set forth in (a) and (b), the implicit solver will be constructed such that it reduces to the dual a scheme if $\mu = 0$. The former differs from the latter only in the extra modeling involving the diffusion-related terms. Note that the presence of viscosity is felt through (i) the diffusion term $-\mu\partial^2 u/\partial x^2$ in Eq. (1.2), and (ii) the spatial diffusion flux component $-\mu\partial u/\partial x$ in the flux vector

$$\vec{h} = (au - \mu\partial u/\partial x,\, u) \tag{3.1}$$

Note that Eq. (1.2) is the differential form of Eq. (2.1) if $\vec{h}$ is defined according to Eq. (3.1). Also, in this paper, any term in Eq. (1.2) or on the right side of Eq. (3.1) is considered to be convection-related if it is not diffusion-related.

To construct the a-$\mu(I1)$ scheme, consider a finite portion of the mesh depicted in Fig. 2 ($J \geq 4$). We assume that (i) $u = u_I(x)$ at $t = 0$, (ii) $u = u_L(t)$ at $x = 0$, and (iii) $u = u_R(t)$ at $x = J\Delta x$, where $u_I(x)$, $u_L(t)$, and $u_R(t)$ are the given initial data, left-boundary data and right-boundary data, respectively. Moreover, for the current case, (i) Ω_1 and Ω_2 are restricted by the conditions $n \geq 0$ and $J \geq j \geq 0$, (ii) $\mathrm{CE}_{\pm}(j,n)$ are not defined if $n = 0$, (iii) $\mathrm{CE}_{-}(j,n)$ is not defined if $j = 0$, and (iv) $\mathrm{CE}_{+}(j,n)$ is not defined if $j = J$. Items (iii) and (iv) imply that *only one conservation condition is associated with a boundary mesh point*. Obviously, the definition of $\mathrm{SE}(j,n)$ also needs to be appropriately modified if $j = 0$, or $j = J$, or $n = 0$.

Eq. (2.2) will still be assumed. We also assume that, for $n = 0, 1, 2, \ldots$,

$$u_0^n = u_L(t^n) \qquad (u_t)_0^n = \dot{u}_L(t^n) \qquad u_J^n = u_R(t^n) \qquad (u_t)_J^n = \dot{u}_R(t^n) \tag{3.2}$$

where $\dot{u}_L(t) \stackrel{\text{def}}{=} du_L(t)/dt$ and $\dot{u}_R(t) \stackrel{\text{def}}{=} du_R(t)/dt$. Thus, only one unknown, i.e., $(u_x)_j^n$, and one conservation condition are associated with a boundary mesh point (j,n).

Furthermore, for an interior mesh point (j,n), we replace Eq. (2.3) with

$$(u_t)_j^n = -a(u_x)_j^n + \frac{\mu}{2\Delta x}\left[(u_x)_{j+1}^n - (u_x)_{j-1}^n\right] \quad J > j > 0 \tag{3.3}$$

Eq. (3.3) is the numerical analogue of the differential condition Eq. (1.2). Eqs. (2.2) and (3.3) imply that, for $J > j > 0$ and $(x,t) \in \mathrm{SE}(j,n)$,

$$u^*(x,t\,;j,n) = u_j^n + (u_x)_j^n(x - x_j) + \left\{\frac{\mu}{2\Delta x}\left[(u_x)_{j+1}^n - (u_x)_{j-1}^n\right] - a(u_x)_j^n\right\}(t - t^n) \tag{3.4}$$

Next, as a result of Eq. (3.1), Eq. (2.5) is replaced by

$$\vec{h}^*(x,t\,;j,n) = (au^*(x,t\,;j,n) - \mu u_x^*(x,t\,;j,n),\, u^*(x,t\,;j,n)) \tag{3.5}$$

Here, for any $(x,t) \in \mathrm{SE}(j,n)$,

$$u_x^*(x,t\,;j,n) \stackrel{\text{def}}{=} \begin{cases} \left[(u_x)_j^n + (u_x)_j^{n+1}\right]/2, & \text{if } t \geq t^n; \\ \left[(u_x)_j^n + (u_x)_j^{n-1}\right]/2, & \text{if } t < t^n. \end{cases} \tag{3.6}$$

Consider any point (x,t) on the line segment joining the mesh points (j,n) and $(j,n-1)$. Then (x,t) belongs to both $\mathrm{SE}(j,n)$ and $\mathrm{SE}(j,n-1)$. According to Eq. (3.6), for this point (x,t),

$$u_x^*(x,t\,;j,n) = u_x^*(x,t\,;j,n-1) = \left[(u_x)_j^n + (u_x)_j^{n-1}\right]/2 \tag{3.7}$$

Thus, *the same numerical diffusion flux component is assigned to the point* (x,t) *regardless of whether it is considered as a point in* $SE(j,n)$ *or a point in* $SE(j,n-1)$, in their region of overlap.

With the above modifications, the a-$\mu(I1)$ scheme is defined by assuming Eq. (2.6). Note that:

(a) At a mesh point $\in \Omega_1(\Omega_2)$, the diffusion-related terms in Eqs. (1.2) and (3.1) are modeled using *interpolations* that may involve the numerical values of the mesh points $\in \Omega_2(\Omega_1)$. *This contrasts sharply with the modeling of the convection-related terms which uses no interpolation.*

(b) In the dual a scheme, the two sets of numerical variables associated with Ω_1 and Ω_2 are completely decoupled from each other. Contrarily, *they are "glued" together in the* a-μ(I1) *scheme through the interpolations referred to in (a).*

To proceed, let $\alpha = \mu\Delta t/(\Delta x)^2$, and $(u_t^+)_j^n \stackrel{\text{def}}{=} (\Delta t/2)(u_t)_j^n$. Also let

$$\begin{aligned}(S_+)_j^n \stackrel{\text{def}}{=}\quad & (1-\nu)u_{j+1}^n + (\frac{\nu}{2}-1)\alpha(u_x^+)_j^n - (1-\nu^2-\alpha)(u_x^+)_{j+1}^n \\ & -\frac{\nu\alpha}{2}(u_x^+)_{j+2}^n \quad (n=0,1,2,\ldots;j=0,1,2,\ldots,J-2)\end{aligned} \tag{3.8}$$

$$(S_+)_{J-1}^n \stackrel{\text{def}}{=} (1-\nu)u_J^n - \alpha(u_x^+)_{J-1}^n - (1-\alpha)(u_x^+)_J^n - \nu(u_t^+)_J^n \quad (n=0,1,2,\ldots) \tag{3.9}$$

$$\begin{aligned}(S_-)_j^n \stackrel{\text{def}}{=}\quad & (1+\nu)u_{j-1}^n + (\frac{\nu}{2}+1)\alpha(u_x^+)_j^n + (1-\nu^2-\alpha)(u_x^+)_{j-1}^n \\ & -\frac{\nu\alpha}{2}(u_x^+)_{j-2}^n \quad (n=0,1,2,\ldots;j=2,3,4,\ldots,J)\end{aligned} \tag{3.10}$$

$$(S_-)_1^n \stackrel{\text{def}}{=} (1+\nu)u_0^n + \alpha(u_x^+)_1^n + (1-\alpha)(u_x^+)_0^n + \nu(u_t^+)_0^n \quad (n=0,1,2,\ldots) \tag{3.11}$$

By using Eqs. (2.2), (3.2), (3.4)–(3.6), and (3.8)–(3.11), Eq. (2.6) implies that

$$\begin{aligned}&(1\mp\nu)u_j^n \pm (1-\nu^2+\alpha)(u_x^+)_j^n + (\frac{\nu}{2}\mp 1)\alpha(u_x^+)_{j\pm1}^n - \frac{\nu\alpha}{2}(u_x^+)_{j\mp1}^n \\ =\ & (S_\pm)_j^{n-1} \quad (n=1,2,3,\ldots;j=1,2,\ldots,J-1)\end{aligned} \tag{3.12}$$

$$(1+\alpha)(u_x^+)_0^n - \alpha(u_x^+)_1^n = (S_+)_0^{n-1} - (1-\nu)u_0^n - \nu(u_t^+)_0^n \quad (n=1,2,\ldots) \tag{3.13}$$

$$\alpha(u_x^+)_{J-1}^n - (1+\alpha)(u_x^+)_J^n = (S_-)_J^{n-1} - (1+\nu)u_J^n + \nu(u_t^+)_J^n \quad (n=1,2,\ldots) \tag{3.14}$$

Eqs. (3.12)–(3.14) define the a-$\mu(I1)$ scheme. Note that Eq. (3.12) represents a pair of equations for each (j,n).

This section is concluded with a discussion of another implicit scheme, referred to as the a-$\mu(I2)$ scheme. It differs from the a-$\mu(I1)$ scheme only in one respect, i.e., Eq. (3.3) is replaced by

$$(u_t)_j^n = -a(u_x)_j^n + \frac{\mu}{(\Delta x)^2}(u_{j+1}^n + u_{j-1}^n - 2u_j^n) \quad J > j > 0 \tag{3.15}$$

As a result, Eq. (3.4) must be modified accordingly. Note that (i) because the a-$\mu(I1)$ and a-$\mu(I2)$ schemes differ only in the representation of the viscous flux in Eqs. (3.3) and (3.15), the two schemes are identical if $\mu = 0$, and (ii) because the differing expressions for $(u_t)_j^n$ in Eqs. (3.3) and (3.15) are applied only in the evaluation of the flux of au^* in the conservation equations, the two schemes are identical if $a = 0$. Let

$$\begin{aligned}(R_+)_j^n \stackrel{\text{def}}{=} \quad & (1-\nu+\nu\alpha)u_{j+1}^n - \alpha(u_x^+)_j^n - (1-\nu^2-\alpha)(u_x^+)_{j+1}^n \\ & -\frac{\nu\alpha}{2}\left(u_j^n + u_{j+2}^n\right) \quad (n = 0,1,2,\ldots;\, j = 0,1,2,\ldots,J-2)\end{aligned} \tag{3.16}$$

$$(R_+)_{J-1}^n \stackrel{\text{def}}{=} (1-\nu)u_J^n - \alpha(u_x^+)_{J-1}^n - (1-\alpha)(u_x^+)_J^n - \nu(u_t^+)_J^n \quad (n = 0,1,2,\ldots) \tag{3.17}$$

$$\begin{aligned}(R_-)_j^n \stackrel{\text{def}}{=} \quad & (1+\nu-\nu\alpha)u_{j-1}^n + \alpha(u_x^+)_j^n + (1-\nu^2-\alpha)(u_x^+)_{j-1}^n \\ & +\frac{\nu\alpha}{2}\left(u_j^n + u_{j-2}^n\right) \quad (n = 0,1,2,\ldots;\, j = 2,3,4,\ldots,J)\end{aligned} \tag{3.18}$$

$$(R_-)_1^n \stackrel{\text{def}}{=} (1+\nu)u_0^n + \alpha(u_x^+)_1^n + (1-\alpha)(u_x^+)_0^n + \nu(u_t^+)_0^n \quad (n = 0,1,2,\ldots) \tag{3.19}$$

Then in the a-$\mu(I2)$ scheme, Eqs. (3.12)–(3.14) are replaced by

$$\begin{aligned}& (1 \mp \nu \mp \nu\alpha)u_j^n \pm (1-\nu^2+\alpha)(u_x^+)_j^n \mp \alpha(u_x^+)_{j\pm1}^n \pm \frac{\nu\alpha}{2}\left(u_{j+1}^n + u_{j-1}^n\right) \\ = \quad & (R_\pm)_j^{n-1} \quad (n = 1,2,3,\ldots;\, j = 1,2,\ldots,J-1)\end{aligned} \tag{3.20}$$

$$(1+\alpha)(u_x^+)_0^n - \alpha(u_x^+)_1^n = (R_+)_0^{n-1} - (1-\nu)u_0^n - \nu(u_t^+)_0^n \quad (n = 1,2,\ldots) \tag{3.21}$$

$$\alpha(u_x^+)_{J-1}^n - (1+\alpha)(u_x^+)_J^n = (R_-)_J^{n-1} - (1+\nu)u_J^n + \nu(u_t^+)_J^n \quad (n = 1,2,\ldots) \tag{3.22}$$

Eqs. (3.20)–(3.22) define the a-$\mu(I2)$ scheme. Note that Eq. (3.20) represents a pair of equations for each (j,n).

4 Solution Procedure

We first discuss the solution procedure of the a-$\mu(I1)$ scheme. Let $1-\nu^2 \neq 0$. Then Eq. (3.12) is equivalent to the pair of equations

$$-\alpha(u_x^+)_{j-1}^n + 2(1-\nu^2+\alpha)(u_x^+)_j^n - \alpha(u_x^+)_{j+1}^n = (1+\nu)(S_+)_j^{n-1} - (1-\nu)(S_-)_j^{n-1} \tag{4.1}$$

and

$$u_j^n = \frac{1}{2}\left\{(S_+)_j^{n-1} + (S_-)_j^{n-1} + \alpha\left[(u_x^+)_{j+1}^n - (u_x^+)_{j-1}^n\right]\right\} \tag{4.2}$$

where $j = 1, 2, 3, \ldots, J-1$. In the following discussion, Eqs. (3.12)–(3.14) will be replaced by Eqs. (3.13), (3.14), (4.1) and (4.2).

Let the marching variables at the $(n-1)$th time level be given. With the aid of Eq. (3.2), the expressions on the right sides of Eqs. (3.13), (3.14) and (4.1) can be considered as given source terms. Thus these equations form a tridiagonal system of $J+1$ equations for the $J+1$ unknowns $(u_x^+)_j^n$, $j = 0, 1, 2, \ldots, J$. It can be shown [6] that the coefficient matrix associated with the tridiagonal system is strictly diagonally dominant in rows and columns, i.e., stability of the Thomas algorithm ([15], p.99) for solving the system is assured, if

$$\nu^2 < 1 \qquad \text{and} \qquad \alpha \geq 0 \tag{4.3}$$

Upon obtaining $(u_x^+)_j^n$, $j = 0, 1, 2, \ldots, J$ by solving the tridiagonal system, the other unknowns u_j^n, $j = 1, 2, \ldots, J-1$, can be obtained using Eq. (4.2). The time-marching stability of the a-$\mu(I1)$ scheme, as well as that of the a-$\mu(I2)$ scheme, is discussed in the next section.

Finally, we briefly discuss the solution procedure of the a-$\mu(I2)$ scheme. If the marching variables at the $(n-1)$th time level and the boundary conditions Eq. (3.2) are given, the expressions on the right sides of Eqs. (3.20)–(3.22) can be considered as given source terms. Thus these equations form a system of equations for the u_j^n and the $(u_x^+)_j^n$ at the nth time level. Unlike the case with the a-$\mu(I1)$ scheme, prior elimination of the u_j^n at each mesh point to obtain a system for only the $(u_x^+)_j^n$ is not possible, as the conservation equations (3.20) are implicit in both u_j^n and $(u_x^+)_j^n$. Hence, the resulting system for the u_j^n and the $(u_x^+)_j^n$ must be solved by a block version of the Thomas algorithm. This makes the a-$\mu(I1)$ scheme computationally more efficient than the a-$\mu(I2)$ scheme.

5 Stability Analysis

Let

$$\vec{q}(j,n) \stackrel{def}{=} \begin{bmatrix} u_j^n \\ (u_x^+)_j^n \end{bmatrix} \tag{5.1}$$

$$Q_{-1}^{(1)} \stackrel{def}{=} \begin{pmatrix} 0 & -\nu\alpha/2 \\ 0 & (\nu/2+1)\,\alpha \end{pmatrix} \tag{5.2}$$

$$Q_0^{(1)} \stackrel{def}{=} \begin{pmatrix} 1-\nu & 1-\nu^2+\alpha \\ 1+\nu & -(1-\nu^2+\alpha) \end{pmatrix} \tag{5.3}$$

$$Q_1^{(1)} \stackrel{def}{=} \begin{pmatrix} 0 & (\nu/2-1)\,\alpha \\ 0 & -\nu\alpha/2 \end{pmatrix} \tag{5.4}$$

$$Q_{-2}^{(2)} \stackrel{def}{=} \begin{pmatrix} 0 & 0 \\ 0 & -\nu\alpha/2 \end{pmatrix} \tag{5.5}$$

$$Q_{-1}^{(2)} \stackrel{def}{=} \begin{pmatrix} 0 & 0 \\ 1+\nu & 1-\nu^2-\alpha \end{pmatrix} \tag{5.6}$$

$$Q_{0}^{(2)} \stackrel{def}{=} \begin{pmatrix} 0 & (\nu/2-1)\,\alpha \\ 0 & (\nu/2+1)\,\alpha \end{pmatrix} \tag{5.7}$$

$$Q_{1}^{(2)} \stackrel{def}{=} \begin{pmatrix} 1-\nu & -(1-\nu^2-\alpha) \\ 0 & 0 \end{pmatrix} \tag{5.8}$$

$$Q_{2}^{(2)} \stackrel{def}{=} \begin{pmatrix} 0 & -\nu\alpha/2 \\ 0 & 0 \end{pmatrix} \tag{5.9}$$

Then Eq. (3.12) may be expressed as

$$\sum_{l=-1}^{1} Q_l^{(1)} \vec{q}(j+l,n) = \sum_{l=-2}^{2} Q_l^{(2)} \vec{q}(j+l,n-1). \tag{5.10}$$

We examine the evolution of a single Fourier mode of the error by making the substitution

$$\vec{q}(j,n) = \vec{q}^{\,*}(n,\theta)\, e^{ij\theta} \qquad (i \equiv \sqrt{-1}, \quad -\pi < \theta \leq \pi) \tag{5.11}$$

in Eq. (5.10), where (i) $\vec{q}^{\,*}(n,\theta)$ is a 2×1 column matrix, and (ii) θ, $-\pi < \theta \leq \pi$, is the phase angle variation per unit Δx of a single Fourier mode. Performing this substitution, we obtain

$$Q^{(1)}(\nu,\alpha,\theta)\, \vec{q}^{\,*}(n,\theta) = Q^{(2)}(\nu,\alpha,\theta)\, \vec{q}^{\,*}(n-1,\theta), \tag{5.12}$$

where

$$\begin{aligned} Q^{(1)}(\nu,\alpha,\theta) &\stackrel{def}{=} \sum_{l=-1}^{1} e^{li\theta} Q_l^{(1)} \\ &= \begin{bmatrix} 1-\nu & 1-\nu^2+\alpha-\frac{\nu\alpha}{2}e^{-i\theta}+\alpha\left(\frac{\nu}{2}-1\right)e^{i\theta} \\ 1+\nu & -(1-\nu^2+\alpha)-\frac{\nu\alpha}{2}e^{i\theta}+\alpha\left(\frac{\nu}{2}+1\right)e^{-i\theta} \end{bmatrix} \end{aligned} \tag{5.13}$$

and

$$\begin{aligned} Q^{(2)}(\nu,\alpha,\theta) &\stackrel{def}{=} \sum_{l=-2}^{2} e^{li\theta} Q_l^{(2)} \\ &= \begin{bmatrix} (1-\nu)e^{i\theta} & -(1-\nu^2-\alpha)\,e^{i\theta}-\frac{\nu\alpha}{2}e^{2i\theta}+\alpha\left(\frac{\nu}{2}-1\right) \\ (1+\nu)e^{-i\theta} & (1-\nu^2-\alpha)\,e^{-i\theta}-\frac{\nu\alpha}{2}e^{-2i\theta}+\alpha\left(\frac{\nu}{2}+1\right) \end{bmatrix}. \end{aligned} \tag{5.14}$$

Because

$$\begin{aligned} \Delta^{(1)}(\nu,\alpha,\theta) &\stackrel{def}{=} \det\left[Q^{(1)}(\nu,\alpha,\theta)\right] \\ &= -2\left[\left(1-\nu^2\right)+\alpha\left(1-\cos\theta\right)\right], \end{aligned} \tag{5.15}$$

it is evident that $\Delta^{(1)} \neq 0$ for $-\pi < \theta \leq \pi$ if the conditions Eq. (4.3) are satisfied. Assuming Eq. (4.3), then $\left[Q^{(1)}\right]^{-1}$ exists and we can multiply Eq. (5.12) from the left by $\left[Q^{(1)}\right]^{-1}$. As a result, the amplification matrix is

$$G(\nu,\alpha,\theta) = \left[Q^{(1)}(\nu,\alpha,\theta)\right]^{-1} Q^{(2)}(\nu,\alpha,\theta). \tag{5.16}$$

The amplification factors of the a-$\mu(I1)$ scheme are the eigenvalues of G. It is straightforward to show that any eigenvalue $\lambda(\nu,\alpha,\theta)$ of $G(\nu,\alpha,\theta)$ satisfies the condition

$$\det\left[Q^{(2)}(\nu,\alpha,\theta) - \lambda Q^{(1)}(\nu,\alpha,\theta)\right] = 0. \tag{5.17}$$

Using the definitions Eqs. (5.13) and (5.14), Eq. (5.17) is equivalent to

$$A\lambda^2 + B\lambda + C = 0, \tag{5.18}$$

where

$$A = \left(1-\nu^2\right) + \alpha\left(1-\cos\theta\right) \tag{5.19}$$

$$B = 2\alpha\left(1-\cos\theta-\nu^2\sin^2\theta\right) + 2i\nu\left(1-\nu^2\right)\sin\theta \tag{5.20}$$

and

$$C = -\left(1-\nu^2\right) + \alpha\left(1-\cos\theta\right). \tag{5.21}$$

Thus, the amplification factors $\lambda_\pm$ are given by

$$\lambda_\pm = \frac{-B \pm \sqrt{B^2-4AC}}{2A}. \tag{5.22}$$

Note that there are two amplification factors rather than one, because there are two unknowns at each mesh point. Also note that (i) $\lambda_\pm \to \pm 1$ and $\theta \to 0$ if $1-\nu^2 \neq 0$, and (ii) the analytical amplification factor of a plane-wave solution to Eq. (1.2) approaches 1 as $\theta \to 0$. Therefore, λ_+ and λ_- are referred to as the principal and spurious amplification factors, respectively. Numerical evaluations of $\lambda_\pm$ have shown that the a-$\mu(I1)$ scheme is stable provided that the conditions Eq. (4.3) are satisfied.

Note that many other implicit solvers are unconditionally stable. However, the price paid for this "desirable" property usually is excessive numerical dissipation. Moreover, the use of a time-step size that is greater than that allowed by Eq. (4.3) generally results in a less accurate time-dependent solution. Thus we do not consider the more restrictive stability condition Eq. (4.3) to be a disadvantage of the a-$\mu(I1)$ scheme.

When $\mu = 0$, the a-$\mu(I1)$ scheme reduces by design to the dual a scheme. Also, Eq. (5.22) implies that

$$\lambda_{\pm} = -i\nu \sin\theta \pm \sqrt{1 - \nu^2 \sin^2\theta} \qquad \text{if } \mu = 0 \tag{5.23}$$

The amplification factors given in Eq. (5.23) are exactly identical to those of the classical Leapfrog scheme ([15], p.100). On the other hand, Eq. (5.22) implies that

$$\lambda_{+} = \frac{1 - \alpha(1 - \cos\theta)}{1 + \alpha(1 - \cos\theta)} \qquad \text{and} \qquad \lambda_{-} = -1 \qquad \text{if } a = 0 \tag{5.24}$$

It is found that in this case λ_+ is identical to the amplification factor of the Crank-Nicolson scheme ([15], p. 112).

The fact that the amplification factors of the a-$\mu(I1)$ scheme are related to those of two celebrated classical schemes is only one among a string of similar coincidences. Other coincidences are summarized in the following remarks [1, 6, 10]:

(a) By using exactly the same procedure by which the dual a scheme is formed from two decoupled a schemes, the dual a-μ scheme and the dual a-ε scheme can be constructed using the a-μ scheme [1] and the a-ε scheme [1], respectively. It can be shown that the amplification factors of the dual a-μ scheme reduce to those of the Leapfrog scheme when $\mu = 0$ and to those of the DuFort-Frankel scheme ([15], p.114) when $a = 0$. Also, it can be shown that the amplification factors of the dual a-ε scheme (i) reduce to those of the Leapfrog scheme when $\varepsilon = 0$, and (ii) become the same function of ν and θ when $\varepsilon = 1$ and this function is identical to the amplification factor of the Lax scheme.

(b) It is explained in [1] that each of the Leapfrog, DuFort-Frankel and Lax schemes is formed by two decoupled schemes (each of the decoupled schemes is defined on a staggered space-time mesh). It is also shown in [1] that the amplification factors of the decoupled Leapfrog, DuFort-Frankel and Lax schemes are related to those of the a, a-μ and a-ε schemes in exactly the same ways that the amplification factors of the Leapfrog, DuFort-Frankel and Lax schemes are related to those of the dual a, a-μ and a-ε schemes

In [6], the stability of the a-$\mu(I2)$ scheme is analysed, with the same procedure as was used for the a-$\mu(I1)$ scheme. It is shown there that the a-$\mu(I2)$ scheme is stable if the conditions Eq. (4.3) are satisfied. As pointed out in Section 3, when $a = 0$, the a-$\mu(I1)$ scheme and the a-$\mu(I2)$ scheme become identical. Hence, the a-$\mu(I2)$ scheme shares with the a-$\mu(I1)$ scheme the property that when $a = 0$, its principal amplification factor becomes identical to the amplification factor of the Crank-Nicolson scheme. Since the a-$\mu(I2)$ scheme also reduces to the dual a scheme when $\mu = 0$, its amplification factors also reduce to those of the Leapfrog scheme in this case.

6 Consistency and Truncation Error

In this section, we discuss the consistency and truncation error of the a-$\mu(I1)$ scheme. For a similar analysis of the a-$\mu(I2)$ scheme, the reader is referred to [6]. As a preliminary, this section will begin with a discussion of a critical concept.

First, note that in a typical numerical scheme, a physical variable is associated with a single numerical variable. Thus, a system of two coupled physical equations involving two independent physical solution variables, at each mesh point generally is modeled by a system of two coupled discrete equations involving two independent numerical variables. Also, one would expect that the two coupled discrete equations are consistent with the two coupled physical equations. Thus, *in general, one would not expect that two coupled discrete equations be consistent with only a single PDE.*

The a-$\mu(I1)$ scheme is nontraditional in one key respect. Even though it is introduced to model a single PDE (i.e., Eq. (1.2)) with a single dependent variable u, at each interior mesh point it is formed by two coupled discrete equations (see Eq. (3.12)) involving two independent numerical variables u_j^n and $(u_x)_j^n$ (note: $(u_x^+)_j^n = \Delta x/2\ (u_x)_j^n$).

The numerical variables u_j^n and $(u_x)_j^n$ could be "interpreted" as the numerical analogues of u and $\partial u/\partial x$, respectively. However, it should be understood that this interpretation is not exact in nature and that *it certainly does not invalidate the fact that u_j^n and $(u_x)_j^n$ are independent numerical variables.* As a result, one would expect that the two equations given in Eq. (3.12) *be consistent with a system of two PDEs with one of them being Eq. (1.2).*

The interior equations of the a-$\mu(I1)$ scheme, Eq. (3.12), represent the results of the evaluation of Eq. (2.6) with the use of Eq. (3.5). Consider the equations obtained by evaluating

$$F_+(j,n) = 0 \tag{6.1}$$

and

$$F_-(j+1,n) = 0 \tag{6.2}$$

These are two distinct conservation equations, although the conservation elements involved occupy the same physical region. The a-$\mu(I1)$ scheme can obviously alternatively be described by specifying these two equations. Linear combinations of these equations are next examined, in order to investigate the consistency of the scheme. Adding the equations symbolized by Eq. (6.1) and Eq. (6.2), and dividing the result by $2\,\Delta x\,\Delta t$, results in

$$[FDE1(u,u_x)]_{j+\frac{1}{2}}^{n-\frac{1}{2}} = 0 \tag{6.3}$$

with $FDE1$ as defined below. Also, subtracting Eq. (6.2) from Eq. (6.1), and dividing the result by $2(1-\nu^2)\,\Delta x^2$, results in

$$[FDE2(u,u_x)]_{j+\frac{1}{2}}^{n-\frac{1}{2}} = 0 \tag{6.4}$$

Here, $FDE1$ and $FDE2$ are defined as

$$
\begin{aligned}
&[FDE1(u,v)]_{j+\frac{1}{2}}^{n-\frac{1}{2}} \stackrel{def}{=} \\
&\frac{1}{2\triangle t}\left[u_{j+1}^{n}-u_{j+1}^{n-1}+u_{j}^{n}-u_{j}^{n-1}\right]+\frac{a}{2\triangle x}\left[u_{j+1}^{n}-u_{j}^{n}+u_{j+1}^{n-1}-u_{j}^{n-1}\right] \\
&-\frac{\mu}{2\triangle x}\left[v_{j+1}^{n}-v_{j}^{n}+v_{j+1}^{n-1}-v_{j}^{n-1}\right] \\
&-\left[\frac{\triangle x}{4\triangle t}-\frac{\nu a}{4}\right]\left[v_{j+1}^{n}-v_{j}^{n}-v_{j+1}^{n-1}+v_{j}^{n-1}\right] \\
&+\frac{\nu\mu}{8\triangle x}\left[v_{j+2}^{n-1}-v_{j}^{n-1}+v_{j+1}^{n}-v_{j-1}^{n}-v_{j+2}^{n}+v_{j}^{n}-v_{j+1}^{n-1}+v_{j-1}^{n-1}\right]
\end{aligned}
\tag{6.5}
$$

$$
\begin{aligned}
&[FDE2(u,v)]_{j+\frac{1}{2}}^{n-\frac{1}{2}} \stackrel{def}{=} \\
&\frac{1}{4}\left[v_{j+1}^{n}+v_{j}^{n}+v_{j+1}^{n-1}+v_{j}^{n-1}\right] \\
&+\frac{\nu\alpha}{4\left(1-\nu^{2}\right)}\left[v_{j+2}^{n}-v_{j}^{n}+v_{j+1}^{n}-v_{j-1}^{n}+v_{j+2}^{n-1}-v_{j}^{n-1}+v_{j+1}^{n-1}-v_{j-1}^{n-1}\right] \\
&-\frac{1}{2\left(1-\nu^{2}\right)\triangle x}\left[u_{j+1}^{n}-u_{j}^{n}+u_{j+1}^{n-1}-u_{j}^{n-1}\right] \\
&-\frac{\nu}{2\left(1-\nu^{2}\right)\triangle x}\left[u_{j+1}^{n}-u_{j+1}^{n-1}+u_{j}^{n}-u_{j}^{n-1}\right]
\end{aligned}
\tag{6.6}
$$

Note that, to emphasize the fact that u_j^n and $(u_x)_j^n$ are two independent marching variables, a new symbol v is introduced in Eqs. (6.5) and (6.6).

Let $\tilde{u}(x,t)$ and $\tilde{v}(x,t)$ be smooth functions. Furthermore, let (i)

$$PDE1(\tilde{u}) \stackrel{def}{=} \frac{\partial\tilde{u}}{\partial t}+a\frac{\partial\tilde{u}}{\partial x}-\mu\frac{\partial^{2}\tilde{u}}{\partial x^{2}} \tag{6.7}$$

$$PDE2(\tilde{u},\tilde{v}) \stackrel{def}{=} \tilde{v}-\frac{\partial\tilde{u}}{\partial x} \tag{6.8}$$

and (ii) $\tilde{u}_j^n \stackrel{def}{=} \tilde{u}\left(j\triangle x, n\triangle t\right)$ and $\tilde{v} \stackrel{def}{=} \tilde{v}\left(j\triangle x, n\triangle t\right)$. Let $[FDE1(\tilde{u},\tilde{v})]_{j+\frac{1}{2}}^{n-\frac{1}{2}}$ and $[FDE2(\tilde{u},\tilde{v})]_{j+\frac{1}{2}}^{n-\frac{1}{2}}$ be considered as the discrete approximations of $[PDE1(\tilde{u})]_{j+\frac{1}{2}}^{n-\frac{1}{2}}$ and $[PDE2(\tilde{u},\tilde{v})]_{j+\frac{1}{2}}^{n-\frac{1}{2}}$, respectively. Then the errors $ER1$ and $ER2$ in these approximations may be defined by

$$[ER1]_{j+\frac{1}{2}}^{n-\frac{1}{2}} \stackrel{def}{=} [FDE1(\tilde{u},\tilde{v})]_{j+\frac{1}{2}}^{n-\frac{1}{2}}-[PDE1(\tilde{u})]_{j+\frac{1}{2}}^{n-\frac{1}{2}} \tag{6.9}$$

$$[ER2]_{j+\frac{1}{2}}^{n-\frac{1}{2}} \stackrel{def}{=} [FDE2(\tilde{u},\tilde{v})]_{j+\frac{1}{2}}^{n-\frac{1}{2}}-[PDE2(\tilde{u},\tilde{v})]_{j+\frac{1}{2}}^{n-\frac{1}{2}} \tag{6.10}$$

With the aid of Taylor expansions, it may be shown that

$$
\begin{aligned}
[ER1]_{j+\frac{1}{2}}^{n-\frac{1}{2}} \;=\; & -\mu\frac{\partial}{\partial x}\left(\tilde{v}-\frac{\partial\tilde{u}}{\partial x}\right)+\frac{\partial^{3}\tilde{u}}{\partial x^{2}\partial t}\frac{\triangle x^{2}}{8}+\frac{\partial^{3}\tilde{u}}{\partial t^{3}}\frac{\triangle t^{2}}{24} \\
&+a\frac{\partial^{3}\tilde{u}}{\partial x^{3}}\frac{\triangle x^{2}}{24}+a\frac{\partial^{3}\tilde{u}}{\partial x\,\partial t^{2}}\frac{\triangle t^{2}}{8}-\mu\frac{\partial^{3}\tilde{v}}{\partial x^{3}}\frac{\triangle x^{2}}{24}-\mu\frac{\partial^{3}\tilde{v}}{\partial x\,\partial t^{2}}\frac{\triangle t^{2}}{8} \\
&+\frac{1}{8}\frac{\partial^{2}\tilde{v}}{\partial x\,\partial t}\left[a^{2}\triangle t^{2}-\triangle x^{2}\right]-a\mu\frac{\partial^{3}\tilde{v}}{\partial x^{2}\partial t}\frac{\triangle t^{2}}{4}+O\left(\triangle^{3}\right)
\end{aligned}
\tag{6.11}
$$

It may similarly be shown that

$$
\begin{aligned}
&[ER2]_{j+\frac{1}{2}}^{n-\frac{1}{2}} \\
= \;& \frac{-\nu\,\Delta t}{(1-\nu^2)\,\Delta x}\left[\frac{\partial \tilde{u}}{\partial t}+a\frac{\partial \tilde{u}}{\partial x}-\mu\frac{\partial^2 \tilde{u}}{\partial x^2}\right]+\frac{2\nu\alpha\,\Delta x}{1-\nu^2}\frac{\partial}{\partial x}\left(\tilde{v}-\frac{\partial \tilde{u}}{\partial x}\right) \\
&+\frac{\partial^2 \tilde{v}}{\partial x^2}\frac{\Delta x^2}{8}+\frac{\partial^2 \tilde{v}}{\partial t^2}\frac{\Delta t^2}{8} \\
&+\frac{\nu\alpha\,\Delta x}{12\,(1-\nu^2)}\left[7\frac{\partial^3 \tilde{v}}{\partial x^3}\Delta x^2+3\frac{\partial^3 \tilde{v}}{\partial x\,\partial t^2}\Delta t^2\right] \\
&-\frac{1}{24\,(1-\nu^2)}\left[\frac{\partial^3 \tilde{u}}{\partial x^3}\Delta x^2+3\frac{\partial^3 \tilde{u}}{\partial x\,\partial t^2}\Delta t^2\right] \\
&-\frac{\nu\,\Delta t}{24\,(1-\nu^2)\,\Delta x}\left[3\frac{\partial^3 \tilde{u}}{\partial x^2\partial t}\Delta x^2+\frac{\partial^3 \tilde{u}}{\partial t^3}\Delta t^2\right]+O\left(\Delta^3\right) \\
&+\frac{\nu\alpha\,\Delta x}{(1-\nu^2)}O\left(\Delta^3\right)-\frac{1}{(1-\nu^2)}O\left(\Delta^3\right)-\frac{\nu\,\Delta t}{(1-\nu^2)\,\Delta x}O\left(\Delta^3\right) \qquad (6.12)
\end{aligned}
$$

In Eqs. (6.11) and (6.12), all derivatives are evaluated at $((j+1/2)\,\Delta x,(n-1/2)\,\Delta t)$. Each symbol $O\left(\Delta^3\right)$ represents an infinite sum of terms, in which derivatives of $\tilde{u}$ or $\tilde{v}$, and the quantities a, μ and $\Delta x^l \Delta t^m$ occur only as factors in the numerator of each term, with $l,m \geq 0$ and $l+m \geq 3$.

Let $\tilde{u}$ and $\tilde{v}$ be a solution of the system of PDEs $PDE1(\tilde{u})=0$ and $PDE2(\tilde{u},\tilde{v})=0$. Then $[FDE1(\tilde{u},\tilde{v})]_{j+\frac{1}{2}}^{n-\frac{1}{2}}$ and $[FDE2(\tilde{u},\tilde{v})]_{j+\frac{1}{2}}^{n-\frac{1}{2}}$ are by definition the truncation errors of the discrete equations (6.3) and (6.4). Because $[PDE1(\tilde{u})]_{j+\frac{1}{2}}^{n-\frac{1}{2}}=0$ and $[PDE2(\tilde{u},\tilde{v})]_{j+\frac{1}{2}}^{n-\frac{1}{2}}=0$, Eqs. (6.9) and (6.10) imply that $[FDE1(\tilde{u},\tilde{v})]_{j+\frac{1}{2}}^{n-\frac{1}{2}}=[ER1]_{j+\frac{1}{2}}^{n-\frac{1}{2}}$ and $[FDE2(\tilde{u},\tilde{v})]_{j+\frac{1}{2}}^{n-\frac{1}{2}}=[ER2]_{j+\frac{1}{2}}^{n-\frac{1}{2}}$. Also, because $[PDE1(\tilde{u})]_{j+\frac{1}{2}}^{n-\frac{1}{2}}=0$ and $[PDE2(\tilde{u},\tilde{v})]_{j+\frac{1}{2}}^{n-\frac{1}{2}}=0$, the first term on the right hand side of Eq. (6.11) and the first two terms on the right hand side of (6.12) vanish. Assume $\nu^2 \neq 1$. Let the rule of mesh refinement be such that $\frac{\Delta t}{\Delta x}$ remains bounded as $\Delta x \to 0$ and $\Delta t \to 0$. This implies that ν and $\alpha\,\Delta x$ also remain bounded. Examination of $ER1$ and $ER2$ then shows that (i) the discrete equations (6.3) and (6.4) of the a-$\mu(I1)$ scheme are consistent with the advection-diffusion equation $PDE1(\tilde{u})=0$ and with $PDE2(\tilde{u},\tilde{v})=0$, and (ii) the scheme is second-order accurate in space and time.

In [6], a similar consistency analysis of the a-$\mu(I2)$ scheme is performed. The conclusion drawn there is that if the rule of mesh refinement is restricted as described in the previous paragraph, the a-$\mu(I2)$ scheme is also consistent with the advection-diffusion equation $PDE1(\tilde{u})=0$ and with $PDE2(\tilde{u},\tilde{v})=0$, and the scheme is also second-order accurate in space and time.

7 Numerical Results

Three test problems will be used to evaluate the accuracy of the a-$\mu(I1)$ scheme. It is shown in [6] that the a-$\mu(I2)$ scheme yields similar results.

7.1 Decaying Traveling Sine Wave

In the first problem, we consider a special case of Eq. (1.2) ($a = 1$ and $\mu = 0.01$) with $0 \leq x \leq 1$ and $t \geq 0$. The initial and boundary condition functions $u_I(x)$, $u_L(t)$ and $u_R(t)$ are defined such that they are consistent with a special solution to Eq. (1.2), i.e.,

$$u = u_e(x,t) \stackrel{\text{def}}{=} \exp(-4\pi^2\mu t)\sin[2\pi(x-at)] \tag{7.1}$$

Let $u_{ex}(x,t) \stackrel{\text{def}}{=} \partial u_e(x,t)/\partial x$. At any time $t = t^n$, let

$$L_1(u) \stackrel{\text{def}}{=} \frac{1}{(J-1)\exp(-4\pi^2\mu t^n)} \sum_{j=1}^{J-1} |u_j^n - u_e(x_j, t^n)| \tag{7.2}$$

$$L_1(u_x) \stackrel{\text{def}}{=} \frac{1}{(J+1)2\pi\exp(-4\pi^2\mu t^n)} \sum_{j=0}^{J} |(u_x)_j^n - u_{ex}(x_j, t^n)| \tag{7.3}$$

$L_1(u)$ and $L_1(u_x)$ are two error norms (per mesh point) which are normalized by the decay factors of $u_e(x,t)$ and $u_{ex}(x,t)$, respectively.

Let $J = 80$ (i.e., $\Delta x = 1/80$) and $\nu = 0.8$ (i.e., $\Delta t = 0.01$). Then a numerical computation yields $L_1(u) = 0.7961 \times 10^{-3}$ at $t = 4$ (i.e., $n = 400$). Through numerical experiments, it has been shown that both $L_1(u)$ and $L_1(u_x)$ at a given time t are reduced by a factor of 4 if both Δx and Δt are reduced by half, confirming the second-order accurate nature of the scheme.

Fig. 5 shows a comparison of the computed solution at $t = 4$ with the exact solution. It also shows the error $u_e(x_j, t^n) - u_j^n$ scaled by the peak magnitude of the exact solution at that time level. It is seen that the maximum error is less than 0.3% of the peak magnitude. The peak magnitude is seen to be just over 0.2.

Fig. 6 shows a comparison of the errors in the solutions obtained with the a-$\mu(I1)$ scheme and the implicit MacCormack scheme ([15]). Both schemes were applied with the same parameters and mesh as described above. It is seen that the current scheme is considerably more accurate than the implicit MacCormack scheme. Refinement of the grid keeping ν constant would actually make the comparison even more favorable. This is because the implicit MacCormack scheme is second-order accurate in space and time only if α is held constant and $\nu \rightarrow 0$ when refining the grid.

7.2 Pure Diffusion

We consider a special case of the convection-diffusion equation with $a = 0$ and $\mu = 1$, in the domain $0 \leq x \leq 1$ and $t \geq 0$. The initial/boundary conditions completing the problem specification are (i) $u(0,t) = u(1,t) = 0$ for $t \geq 0$, (ii) $u(x,0) = 2x$ for $0 \leq x \leq 0.5$, and (iii) $u(x,0) = 2(1-x)$ for $0.5 \leq x \leq 1$. The solution $u(x,t)$ exhibits the diffusive decay of the initial sawtooth shape. An exact series solution is available, see for e.g. p.15 of [16]. For the CE/SE computation, uniform mesh intervals $\Delta x = 0.02$ and $\Delta t = 0.005$ are used. Fig. 7 shows the time-slice at $t = 0.05$, comparing numerical and exact solutions, and also

showing the error scaled with the peak exact value at that time level. The maximum error magnitude is seen to be about 0.5% of the peak solution value. At $t = 1$ (not shown), when the peak solution value has dwindled to about 4×10^{-5}, the maximum error magnitude is about 0.15% of the peak solution value.

The same problem on the same mesh was solved with the Crank-Nicolson scheme, which is probably the best traditional scheme for the parabolic pure diffusion equation. Fig. 8 shows a comparison between the current scheme and the Crank-Nicolson scheme, at $t = 0.05$. The schemes are seen to be of similar accuracy, as is to be expected from the fact that, when $a = 0$, the principal amplification factor of the a-$\mu(I1)$ scheme is identical to the amplification factor of the Crank-Nicolson scheme.

7.3 Steady State Boundary Layer

We next consider the problem defined for the convection-diffusion equation in the domain $0 \leq x \leq 1$ and $t \geq 0$ by the conditions (i) $u(0,t) = 0$ for $t \geq 0$, (ii) $u(1,t) = 1$ for $t \geq 0$, and (iii) $u(x,0) = x$ for $0 \leq x \leq 1$. The 'steady-state' or time-asymptotic limit of the solution is $u(x,\infty) = [\exp(ax/\mu) - 1] \,/\, [\exp(a/\mu) - 1]$.

The case $a = 1$, $\mu = 0.01$ is selected, so that the 'Reynolds' number $Re = a/\mu = 100$. This leads to the formation of a fairly sharp boundary layer, because the thickness of the layer scales as the inverse of the Reynolds number. Uniform mesh intervals $\Delta x = 0.0025$ and $\Delta t = 0.002$ are used, so that the Courant number is 0.8. Fig. 9 shows the computed and exact steady-state limits, together with the error. The boundary layer is seen to be well resolved, with the maximum magnitude of the error being about 1% of the solution peak.

8 Conclusions and Discussions

In the explicit a-μ scheme [1, 10], the diffusion term in Eq. (1.2) is not modeled, i.e., Eq. (2.3) is assumed. Also the diffusion term in Eq. (3.1) is modeled with no interpolation or extrapolation, with a resulting reduction of time-accuracy. Obviously, such a solver can be used only when the diffusion term is small compared with the convection term. Contrarily, the diffusion terms in both Eqs. (1.2) and (3.1) are modeled in the current implicit solvers.

The current implicit solvers are carefully constructed so that they become identical to the explicit dual a scheme for the pure convection equation, when the viscosity coefficient vanishes. Because the dual a scheme is nondissipative, this construction ensures that the physical dissipation is never overwhelmed by numerical dissipation in the present implicit solvers.

The implicit schemes have been shown to be stable provided the Courant number does not exceed unity in magnitude. There is no dependence of the stability of the schemes on the viscosity parameter, other than the condition that $\mu \geq 0$. Stability analysis reveals the remarkable facts that (i) if $\mu = 0$, the amplification factors of the dual-mesh implicit schemes reduce to those of the classical Leapfrog scheme, and (ii) if $a = 0$, one of the amplification factors of the implicit a-μ schemes reduces to that of the classical Crank-Nicolson scheme.

The truncation error analysis of the discretized equations of the implicit schemes shows that, if the Courant number remains bounded when refining the space-time mesh, they are

consistent with the convection-diffusion equation, and are second-order accurate in space and time.

Numerical examples have borne out the conclusions of the stability and truncation error analysis. The current implicit schemes were seen from the numerical examples to enable stable accurate computations over the whole viscosity range, from the pure diffusion case to convection dominated problems.

References

[1] S.C. Chang, *J. Comput. Phys.*, **119** (1995), pp. 295-324.

[2] S.C. Chang, X.Y. Wang and C.Y. Chow, "The Space-Time Conservation Element and Solution Element Method : A New High-Resolution and Genuinely Multidimensional Paradigm for Solving Conservation Laws", *J. Comput. Phys.*, **156** (1999), pp. 89-136.

[3] S.C. Chang, S.T. Yu, A. Himansu, X.Y. Wang, C.Y. Chow, and C.Y. Loh, "The Method of Space-Time Conservation Element and Solution Element — A New Paradigm for Numerical Solution of Conservation Laws", *Computational Fluid Dynamics Review 1998, Vol. 1*, M.M. Hafez and K. Oshima, eds., World Scientific, Singapore, publ.

[4] X.Y. Wang and S.C. Chang, "A 2D Non-Splitting Unstructured Triangular Mesh Euler Solver Based on the Space-Time Conservation Element and Solution Element Method", *Computational Fluid Dynamics J.*, 8(2), pp. 309–325 (1999).

[5] S.C. Chang, X.Y. Wang, C.Y. Chow and A. Himansu, "The Method of Space-Time Conservation Element and Solution Element – Development of a New Implicit Solver", Proceedings of the Ninth International Conference on Numerical Methods in Laminar and Turbulent Flow, July 10-14, 1995, Atlanta, GA. Also published as NASA TM 106897.

[6] S.C. Chang and A. Himansu, "The Implicit and Explicit a-μ Schemes," NASA/TM—97–206307, November 1997.

[7] S.C. Chang and W.M. To, "A New Numerical Framework for Solving Conservation Laws – The Method of Space-Time Conservation Element and Solution Element", NASA TM 104495, August 1991.

[8] S.C. Chang, "On an Origin of Numerical Diffusion: Violation of Invariance Under Space-Time Inversion", Proceedings of the 23rd Modeling and Simulation Conference, April 30 - May 1, 1992, Pittsburgh, PA, William G. Vogt and Marlin H. Mickle eds., Part 5, pp. 2727-2738. Also published as NASA TM 105776.

[9] S.C. Chang and W.M. To, "A Brief Description of a New Numerical Framework for Solving Conservation Laws – The Method of Space-Time Conservation Element and Solution Element", Proceedings of the 13th International Conference on Numerical

Methods in Fluid Dynamics, July 6-10, 1992, Rome, Italy, M. Napolitano and F. Sabetta, eds., Lecture Notes in Physics 414, Springer-Verlag, pp. 396-400 Also published as NASA TM 105757.

[10] S.C. Chang, "New Developments in the Method of Space-Time Conservation Element and Solution Element - Applications to the Euler and Navier-Stokes Equations", Presented at the Second U.S. National Congress on Computational Mechanics, August 16-18, 1993, Washington D.C. Published as NASA TM 106226.

[11] X.Y. Wang, C.Y. Chow and S.C. Chang, "Application of the Space-Time Conservation Element and Solution Element Method to Shock-Tube Problem", NASA TM 106806, December 1994.

[12] S.C. Chang, X.Y. Wang and C.Y. Chow, "New Developments in the Method of Space-Time Conservation Element and Solution Element – Applications to Two-Dimensional Time-Marching Problems", NASA TM 106758, December 1994.

[13] X.Y. Wang, C.Y. Chow and S.C. Chang, "Application of the Space-Time Conservation Element and Solution Element Method to Two-Dimensional Advection-Diffusion Problems", NASA TM 106946, June 1995.

[14] S.C. Chang, X.Y. Wang and C.Y. Chow, "The Method of Space-Time Conservation Element and Solution Element – Applications to One-Dimensional and Two-Dimensional Time-Marching Flow Problems", AIAA Paper 95-1754, in A Collection of Technical Papers, 12th AIAA CFD Conference, June 19-22, 1995, San Diego, CA, pp. 1258-1291. Also published as NASA TM 106915.

[15] D.A. Anderson, J.C. Tannehill and R.H. Pletcher, *Computational Fluid Mechanics and Heat Transfer*, 1984. Hemisphere Publ. Corp., New York.

[16] G.D. Smith, *Numerical Solution of Partial Differential Equations: Finite Difference Methods*, 3rd ed., 1985. Oxford Univ. Press, New York.

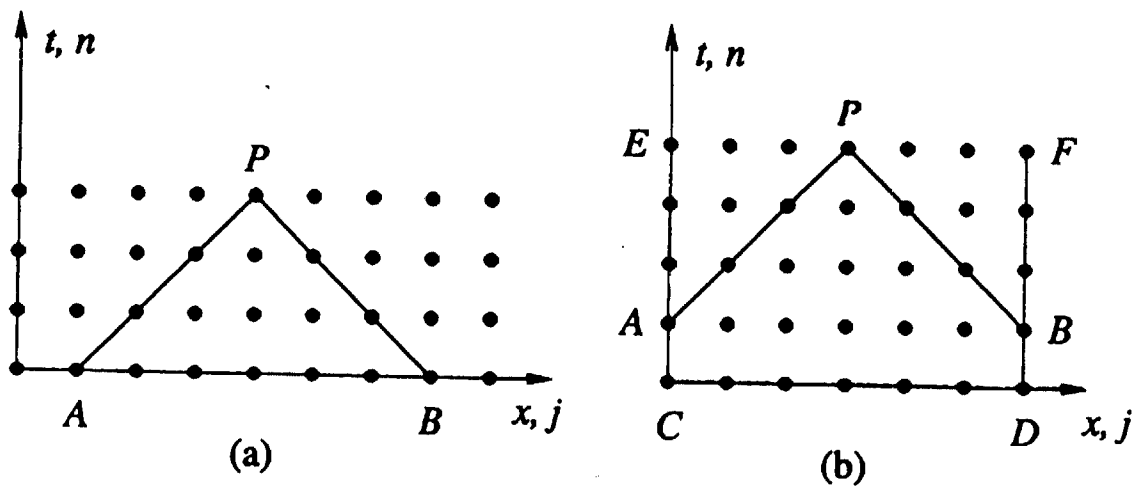

Figure 1 — (a) an initial-value problem
(b) an initial-value/boundary-value problem

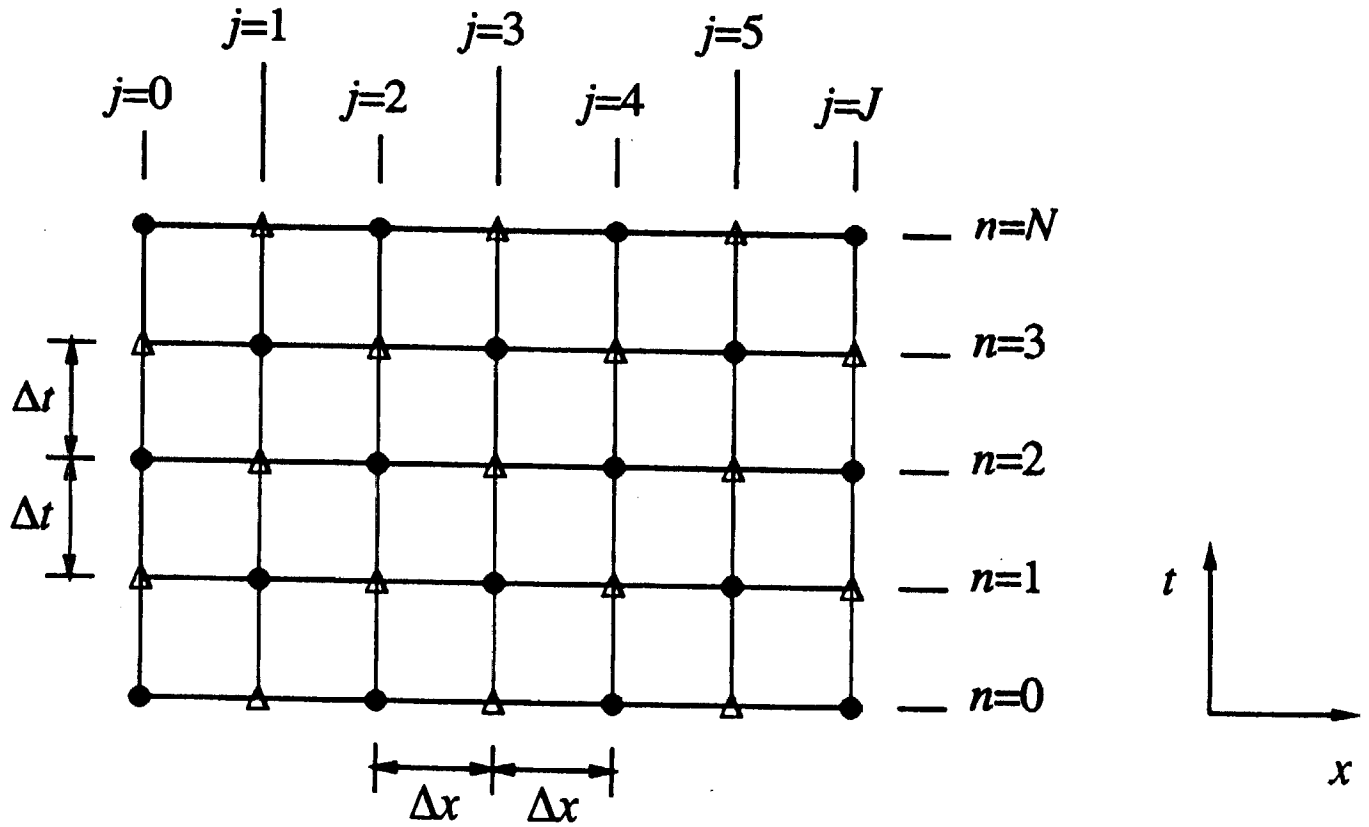

Figure 2 — The space-time mesh of the implicit schemes

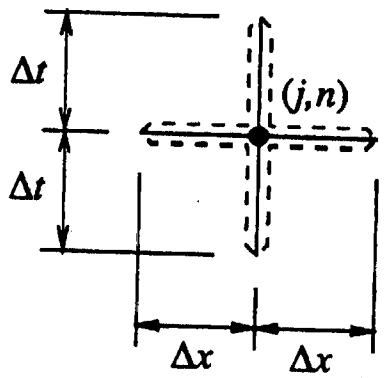

Figure 3 — SE(j,n)

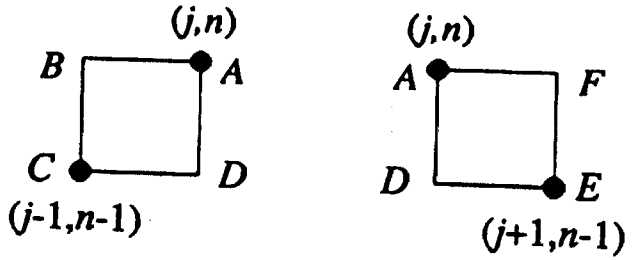

(a) $CE_{-}(j,n)$ (b) $CE_{+}(j,n)$

Figure 4 — The CEs associated with the mesh point (j,n)

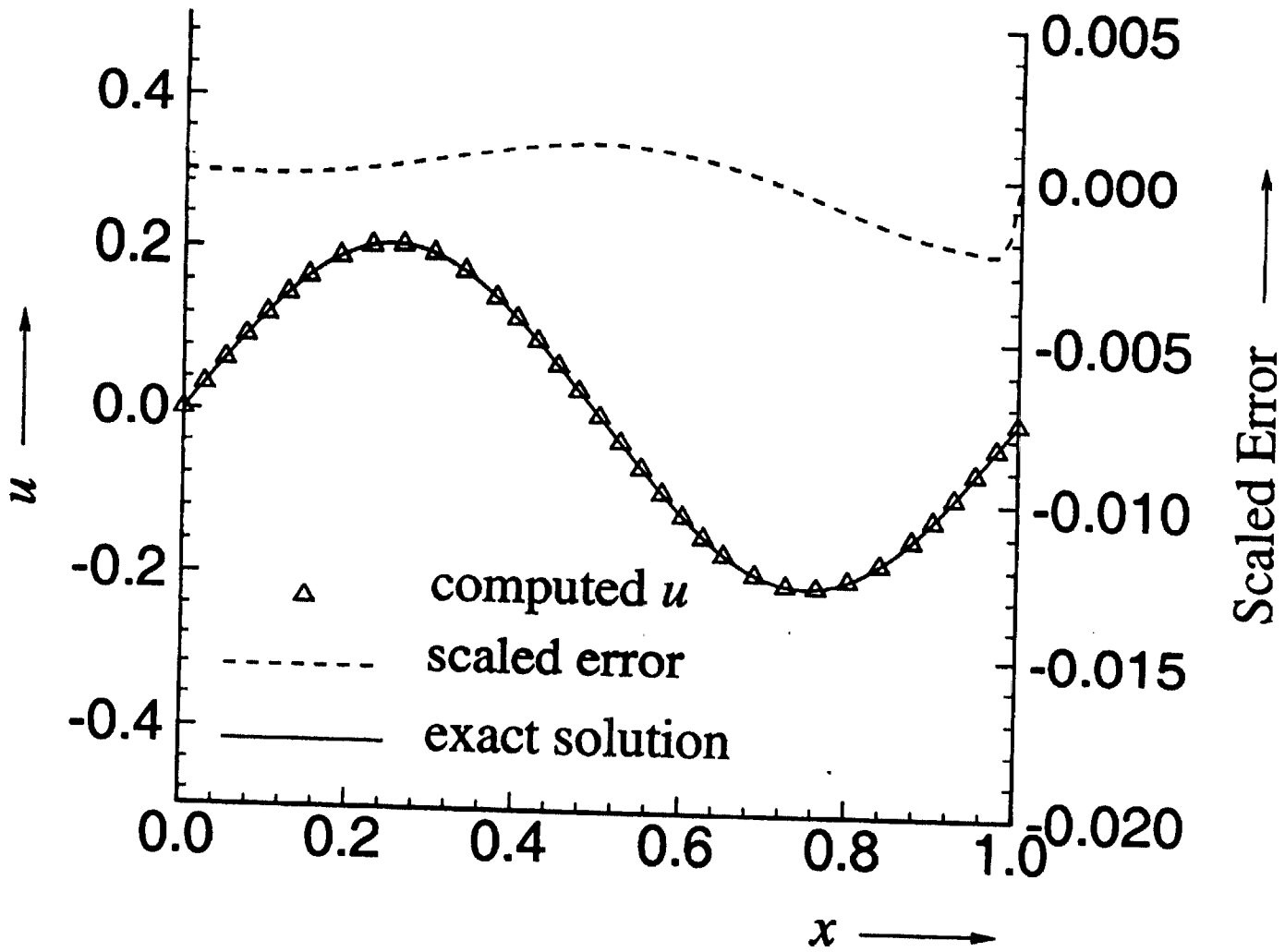

Figure 5 — a-μ ($I1$) Scheme : Sine Wave Example

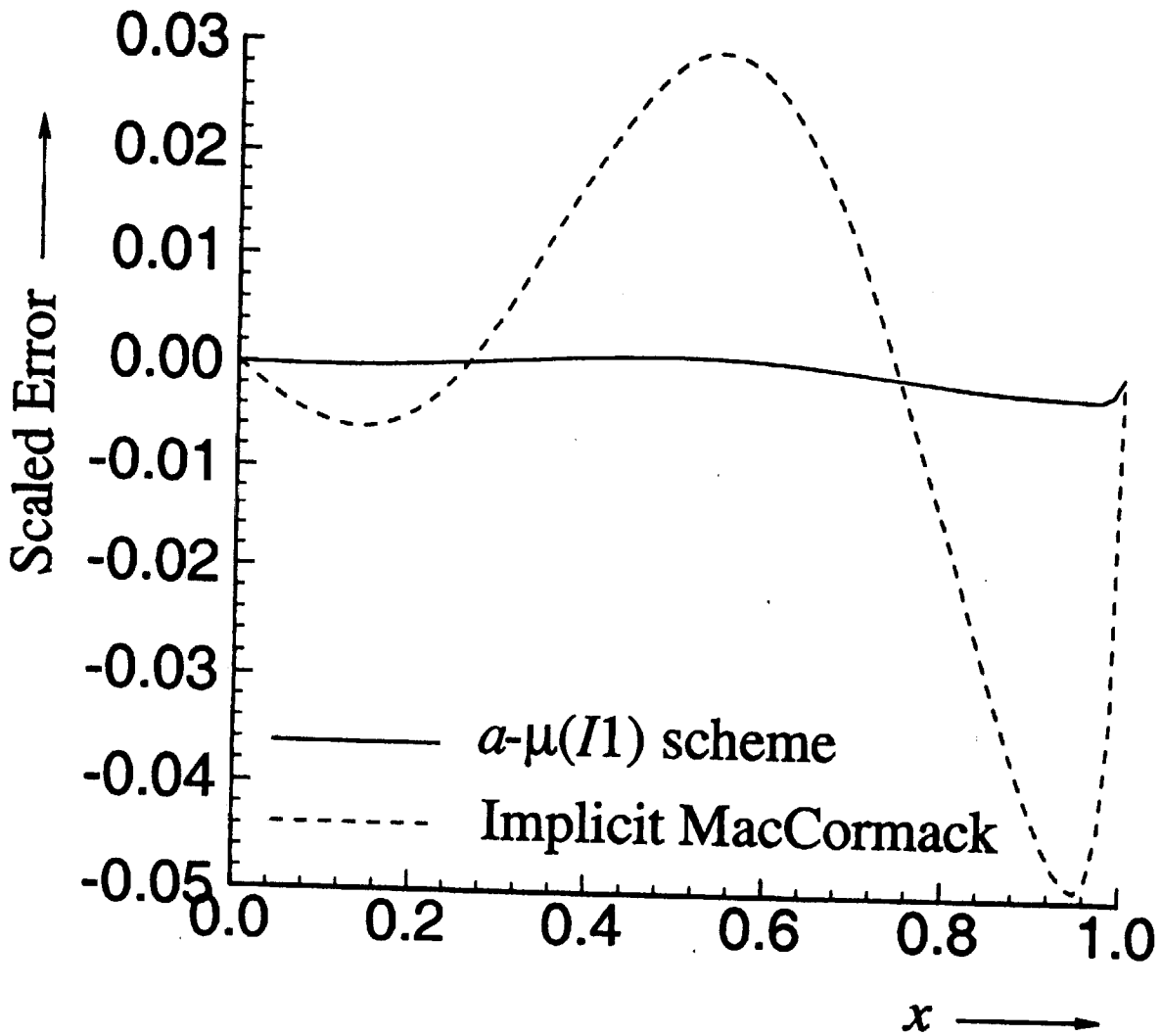

Figure 6 — Sine Wave Example : Comparison of Schemes

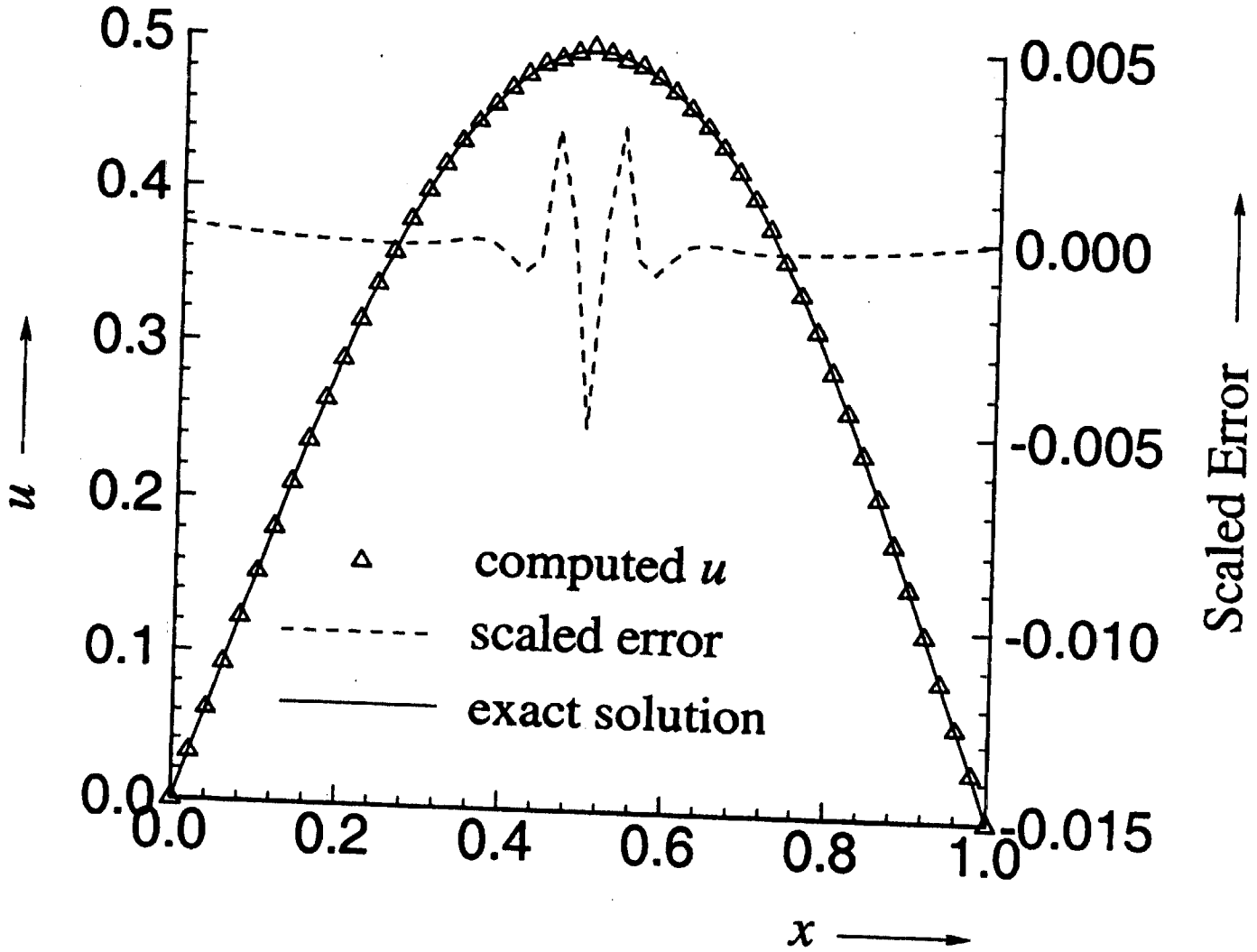

Figure 7 — a-μ ($I1$) Scheme : Pure Diffusion Example

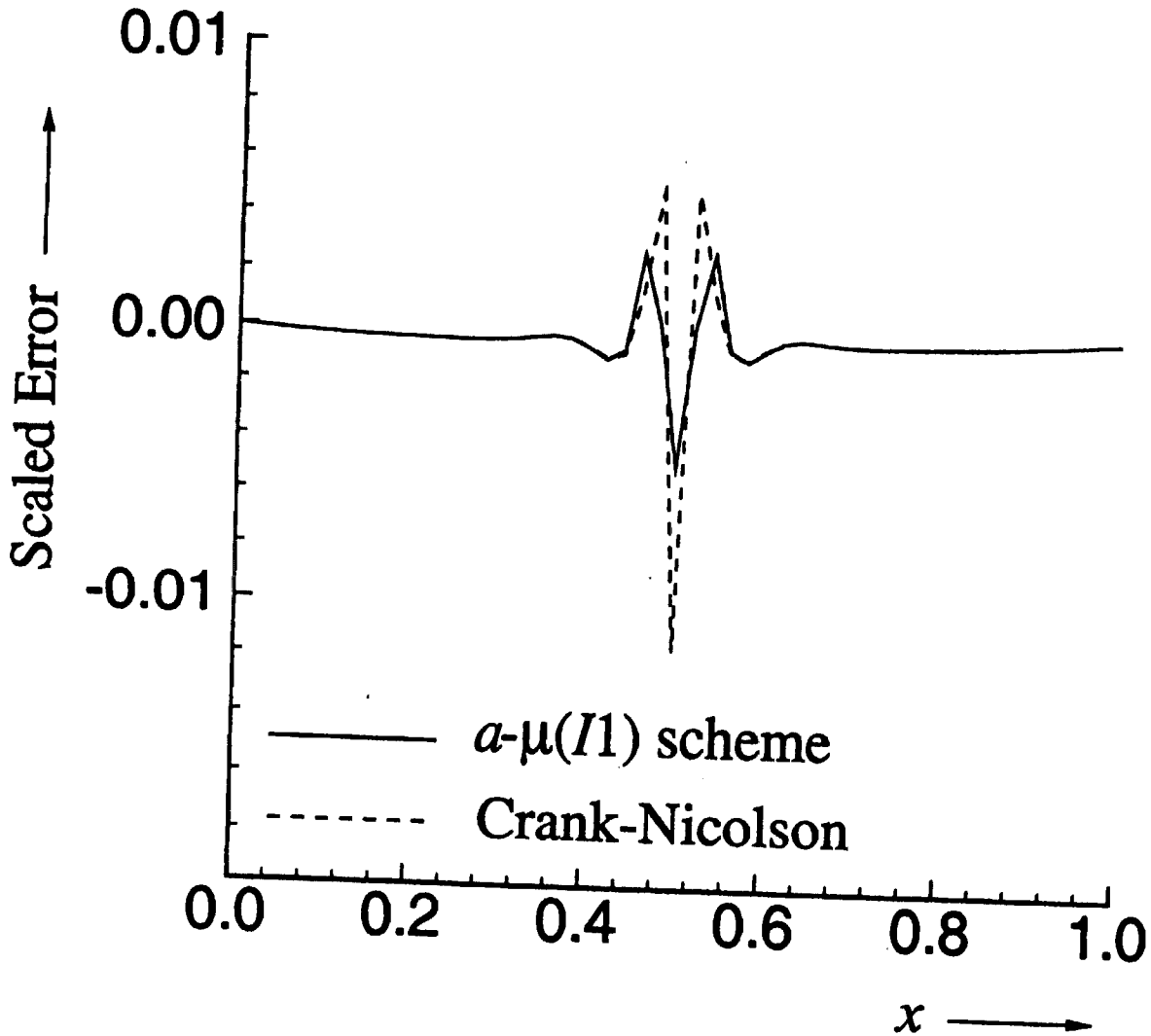

Figure 8 — Pure Diffusion : Comparison of Schemes

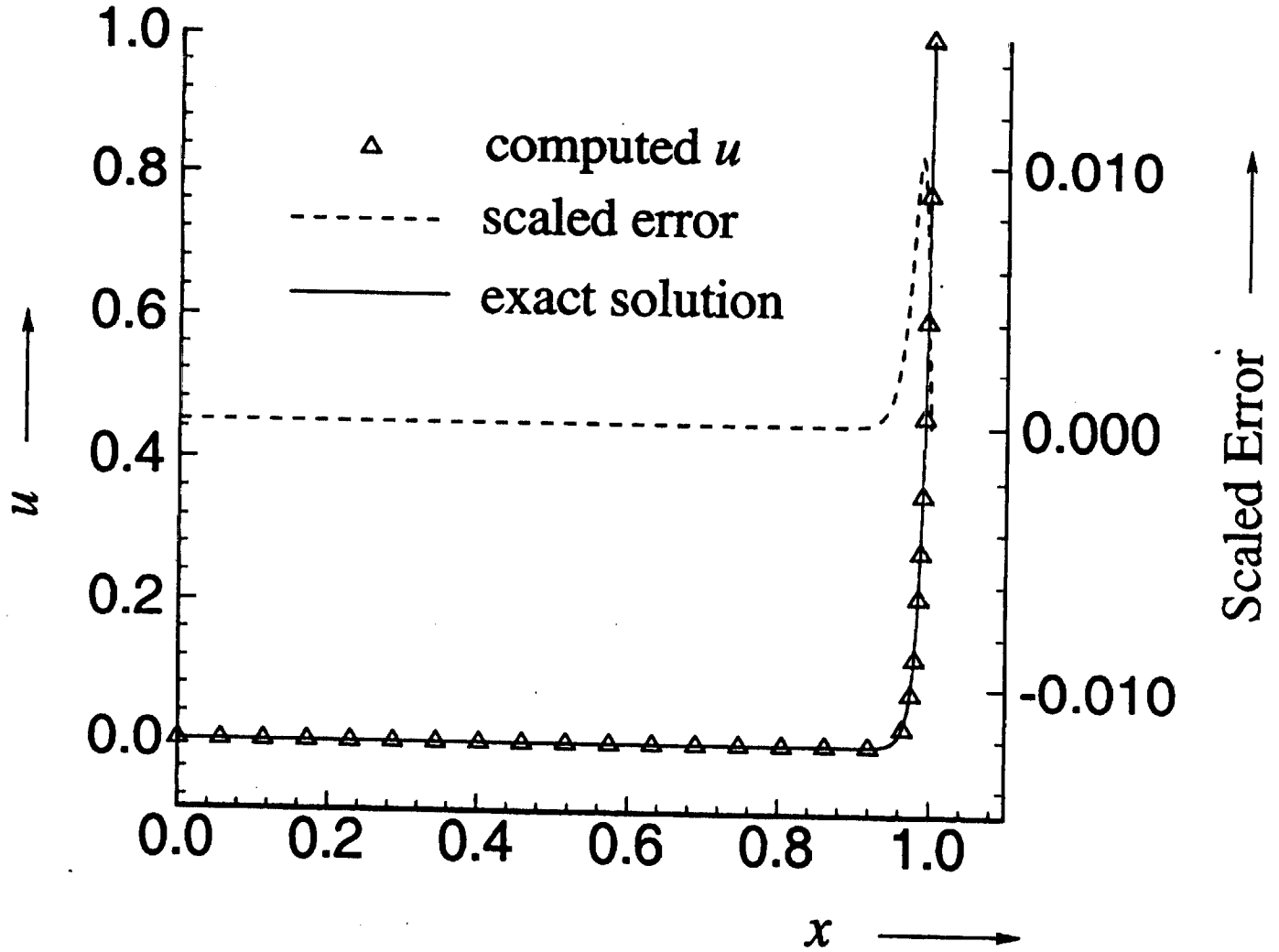

Figure 9 — a-μ ($I1$) Scheme : Boundary Layer, $Re = 100$